

Article

Structural Characterization of Febuxostat/L-Pyroglutamic Acid Cocrystal Using Solid-State ^{13}C -NMR and Investigational Study of Its Water Solubility

Ji-Hun An ^{1,†} , Changjin Lim ^{1,†}, Hyung Chul Ryu ², Jae Sun Kim ², Hyuk Min Kim ², Alice Nguvoko Kiyonga ¹, Minhoo Park ¹, Young-Ger Suh ¹, Gyu Hwan Park ^{3,*} and Kiwon Jung ^{1,*} 

¹ College of Pharmacy, CHA University, Sungnam 13844, Korea; ajh@chauniv.ac.kr (J.-H.A.); koryoi0709@gmail.com (C.L.); gabriella@chauniv.ac.kr (A.N.K.); minho.park92@gmail.com (M.P.); ygsuh@cha.ac.kr (Y.-G.S.)

² R&D Center, J2H biotech, Ansan 15426, Korea; daman-ryu@j2hbio.com (H.C.R.); jsbach@j2hbio.com (J.S.K.); fameoflove@j2hbio.com (H.M.K.)

³ College of Pharmacy, Kyungpook National University, Daegu 41566, Korea

* Correspondence: park014@knu.ac.kr (G.H.P.); pharmj@cha.ac.kr (K.J.); Tel.: +82-53-9508576 (G.H.P.); +82-31-8817173 (K.J.)

† These authors contributed equally to this work.

Academic Editors: Srinivasulu Aitipamula and Reginald Tan

Received: 31 October 2017; Accepted: 5 December 2017; Published: 8 December 2017

Abstract: Febuxostat (FB) is a poorly water-soluble drug that belongs to BCS class II. The drug is employed for the treatment of inflammatory disease arthritis urica (gout), and the free base, FB form-A, is most preferred for drug formulation. In order to achieve a goal of improving the water solubility of FB form-A, this study was carried out using the cocrystallization technique called the liquid-assisted grinding method to produce FB cocrystals. Here, five amino acids containing amine (NH), oxygen (O), and hydroxyl (OH) functional groups, and possessing difference of pKa less than 3 with FB, were selected as cofomers. Then, solvents including methanol, ethanol, isopropyl alcohol, n-hexane, dichloromethane, and acetone were used for the cocrystal screening. As a result, a cocrystal was obtained when acetone and L-pyroglutamic acid (PG) of 0.5 eq. were employed as solvent and cofomer, respectively. The ratio of 2:1, which is the ratio of FB to PG within FB-PG cocrystal, was predicted by means of solid-state CP/MAS ^{13}C -NMR, solution-state NMR (^1H , ^{13}C , and 2D) and FT-IR. Moreover, Powder X-ray Diffraction (PXRD), Differential Scanning Calorimetry (DSC), and Thermogravimetric Analysis (TGA) were used to investigate the characteristics of FB-PG cocrystal. In addition, comparative solubility tests between FB-PG cocrystal and FB form-A were conducted in deionized water and under simulated gastrointestinal pH (1.2, 4, and 6.8) conditions. The result revealed that FB-PG cocrystal has a solubility of four-fold higher than FB form-A in deionized water and two-fold and five-fold greater than FB form-A at simulated gastrointestinal pH 1.2 and pH 4, respectively. Besides, solubilities of FB-PG cocrystal and FB form-A at pH 6.8 were similar to the results measured in deionized water. Therefore, it is postulated that FB-PG cocrystal has a potential overcoming the limitations related to the low aqueous solubility of FB form-A. Accordingly, FB-PG cocrystal is suggested as an alternative active pharmaceutical ingredient of the currently used FB form-A.

Keywords: Febuxostat; cocrystal; solid-state NMR; solubility; active pharmaceutical ingredient

1. Introduction

Most active pharmaceutical ingredients (APIs) are developed in a solid form. The therapeutic efficacies of APIs are optimized or inhibited depending on the type of solid forms selected. Different solid forms can present distinct dissolution rates and solubility, which are two important factors influencing drug bioavailability [1,2]. Cocrystals are solid materials produced by the intermolecular interactions occurring between the former and cofomer, and have an influence in the solid material's crystal structure. Accordingly, the formation of cocrystal is assumed to enhance the drug's solubility and the dissolution rate [3,4].

Cocrystals are solid materials resulting from various stoichiometric (AB, AB₂, A₂B, etc.) ratios between formers and cofomers. These compounds include cocrystal polymorphs, solvates, hydrates, and salts [2]. Functional groups, such as acid...acid, acid...pyridine, acid...amide, amide...amide, amide...pyridine N-oxide, O-H...O, O-H...N, NH...O, and N-H...N, are important factors for designing cocrystals of APIs in constructing the intermolecular hydrogen bondings [5–8]. Moreover, apart from being an important factor in determining the degree of proton transfer, pK_a also influences the occurrences of ionic bonding between formers and cofomers. Hence, maintaining pK_a difference of less than 3 is required for designing cocrystals [2]. Cocrystallization methods including solvent evaporation, solid-state grinding, slurry, solvent drop, supercritical fluid, and the use of anti-solvent have been widely applied to produce cocrystals [9].

The solid-state NMR is an analytical technique used for determining the crystal structure of materials. This technique plays a bridge role between the powder X-ray diffraction (PXRD) and the single crystal X-ray diffraction (SCXRD) analytical techniques, and provides information regarding the solid's conformation as well as the intermolecular interactions occurring within the solid material through the NMR spectrum chemical shifts [10]. This analytical technique is especially useful for predicting the conformations and intermolecular interactions of cocrystals and which single crystals could not be obtained or as supplemental data for the crystal structure determination results achieved by SCXRD analysis. In 2008, by using the solid-state NMR analysis, Vogt et al. [11] determined the intermolecular interactions of cocrystals obtained from a combination where APIs were employed as formers. Moreover, Mandala et al. [12] monitored the formation process of caffeine/malonic acid (2:1) cocrystal by means of solid-state ¹³C-NMR. Another research study suggesting the preparation of cocrystal using APIs, etenzamide and gentisic acid was also reported. The same study predicted the structure of obtained cocrystal using the solid-state NMR analysis and then investigated the cocrystal's dissolution rate [13]. Likewise, the interpretation of the solid-state NMR spectrum chemical shifts is widely applied to ascertain the cocrystal's structure or to investigate the intermolecular interactions occurring within the solid material.

Febuxostat (FB), a xanthine oxidase inhibitor, is a drug that is employed for the treatment of inflammatory disease arthritis urica (gout). Arthritis urica is characterized by the crystallization and accumulation of uric acid in articular cartilage, tendons, and surrounding tissues due to increased uric acid levels in the blood [14]. According to the IUPAC system, the scientific name of FB is 2-(3-cyano-4-isobutoxyphenyl)-4-methyl-1,3-thiazole-5-carboxylic acid (Figure 1a).

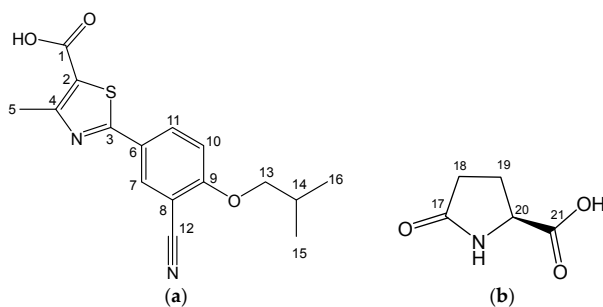


Figure 1. Molecular structure with atom numbers: (a) Febuxostat; (b) L-Pyroglutamic acid.

To date, a total of six FB polymorphs, including five ansoolvates and one methanol solvate, have been reported [15,16]. Of all polymorphs, FB form-A is currently used in the drug formulation. The FB drug is characterized by low aqueous solubility of 0.0129 mg/mL and is restricted to class II according to the Biopharmaceutics Classification System (BCS) [17]. Owing to its low water solubility, FB possesses a very low absorption rate. Therefore, in order to improve its solubility, a study presented five cocrystals formed by the combination of FB and urea, acetamide, nicotinamide, *p*-aminobenzoic acid, and saccharin, then evaluated the dissolution rate of the obtained cocrystals and FB form-A in 60% ethanol-water [17]. In addition, a different study involving the determination of the crystal structure of cocrystal produced from the combination of FB and acetic acid in 1:1 ratio was reported [18]. However, research involving the production of FB cocrystals for improving the water-solubility is yet insignificant.

Accordingly, this study reports the structural characterization of FB/L-Pyroglutamic acid (PG, Figure 1b) (2:1) cocrystal achieved using solid-state CP/MAS ¹³C-NMR and a comparative solubility evaluation of FB-PG (2:1) cocrystal and FB form-A in deionized water and under simulated gastrointestinal pH (1.2, 4, and 6.8) conditions.

2. Results and Discussion

2.1. Cocrystal Screening of Febuxostat

For the purpose of resolving the problem of FB form-A, five amino acids containing hydrophilic NH, O, and OH groups and possessing difference of pKa less than 3 with FB pKa (3.42) were selected. Methanol (MeOH), ethanol (EtOH), isopropyl alcohol (IPA), n-hexane (Hex), dichloromethane (DCM), and acetone (ACT) were utilized as solvents, and the cocrystallization technique of liquid-assisted grinding was applied for FB cocrystals screening (Table 1).

Table 1. Amino acids used as coformer and their pKa.

Coformer	pKa [19]
L-Glutamic acid (1 eq.)	2.19
L-Lysine (1 eq.)	2.16
L-Aspartic acid (1 eq.)	1.88
L-Pyroglutamic Acid (PG) (1 eq.)	3.32
L-Arginine (1 eq.)	2.18

As a result of cocrystal screening, when PG composition was 1 equivalent (eq.), endothermic peak related to FB form-A (endothermic temperature 209.97 °C (Figure S1)) was not observed, but endothermic peak related to PG (endothermic temperature 158.14 °C (Figure S2) [19]) was observed on the DSC curve of FB/PG solid mixture obtained from ACT. However, a new endothermic peak was observed at 194 °C. Nevertheless, no endothermic peak was observed on the DSC curves when other amino acids depicted on Table 1 were utilized for cocrystal screening experiment. The presence of an endothermic peak on the PG's DSC curve is attributed to the pKa difference between PG and FB compared to other amino acids. The difference in pKa between FB 3.42 and PG 3.32, the former/coformer was found very low. Nevertheless, the pKa difference between FB and other amino acids exceeded 1. Therefore, the relatively high acidity of these amino acids compared to PG is assumed to influence their intermolecular interaction with FB and consequently to hinder the formation of cocrystal. Based on the results, FB 1.0 eq. was mixed with 0.1, 0.3, 0.5, 0.8, and 1.0 eq. of PG, respectively, and the obtained solid mixtures were analyzed by using DSC (heating rate 10 °C/min, temperature range 40–250 °C). The endothermic peak related to FB form-A (endothermic temperature 207–208 °C [17]) was not observed on the DSC curves of the solid mixture obtained when PG was 0.5, 0.8, and 1.0 eq. (Figure 2). Consequently, FB-PG cocrystal of 2:1 ratio was produced by means of the liquid-assisted grinding method using ACT as solvent at constant PG composition of 0.5 eq.

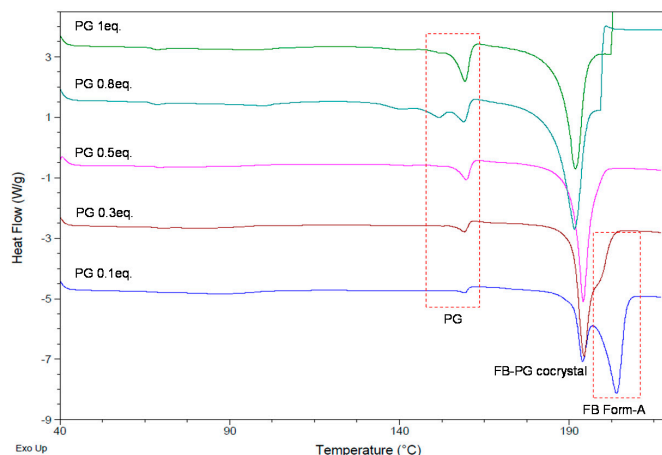


Figure 2. Differential scanning calorimetry (DSC) curves of febusostat (FB)/L-pyroglutamic acid (PG) solid mixtures obtained under PG composition (equivalent) change (heating rate: 10 °C/min, Temperature range: 40–250 °C).

Several attempts have been made to produce single crystal of FB-PG (2:1) cocrystal, however, they were all unsuccessful and no single FB-PG (2:1) cocrystal could be produced. Therefore, the solid-state CP/MAS ^{13}C -NMR, solution-state NMR (^1H , ^{13}C , and 2D), and FT-IR were used to predict the intermolecular interactions of FB-PG cocrystal. Moreover, FB-PG cocrystal characterization was achieved by means of PXRD, DSC, and TGA analysis. The comparative study of the solubility of FB-PG (2:1) cocrystal and FB form-A in deionized water and under simulated gastrointestinal pH (1.2, 4, and 6.8) was performed using HPLC in order to investigate the possibilities of improving water solubility of the FB drug.

2.2. FB-PG Cocrystal Characterization

Figure 3 represents the TGA-DSC curves for FB form-A and PG as well as FB-PG cocrystal. An endothermic peak was observed at 209.97 °C for FB form-A. The DSC endothermic peak of PG appears at 158.14 °C, while the endothermic peak of FB-PG cocrystal was observed at 194.78 °C. According to the same result, no change in mass caused by the solvent or moisture content was noticed. However, decomposition around approximately 200 °C for all crystals was observed.

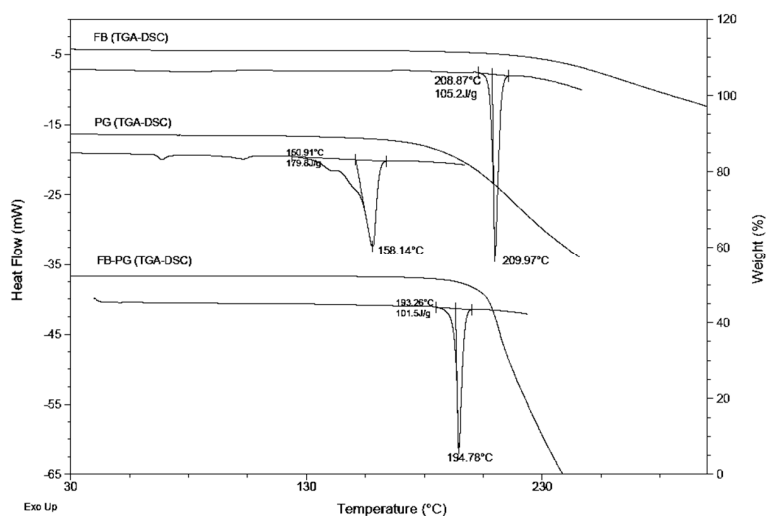


Figure 3. TGA-DSC curves of FB form-A, PG, and FB-PG cocrystal (heating rate 10 °C/min).

Moreover, PXRD analysis was performed to determine the specific characterization of FB-PG cocrystal (Figure 4). The PXRD 2θ angle of FB-PG cocrystal could be observed at 6.9° , 7.42° , 8.45° , 9.94° , 14.5° , 16.65° , and 19.6° ; comparative data with previously reported 2θ PXRD values of FB polymorphs are depicted in Table S1. Contrary to these formerly studied FB polymorphs, FB-PG cocrystal has a distinct PXRD 2θ pattern. Moreover, as observed in Figure 4, FB-PG cocrystal possesses dissimilar 2θ angle with FB form-A and PG crystals (Table S2). Therefore, it can be concluded based on the PXRD data that the FB-PG cocrystal has a different crystal structure compared to FB form-A and PG crystals.

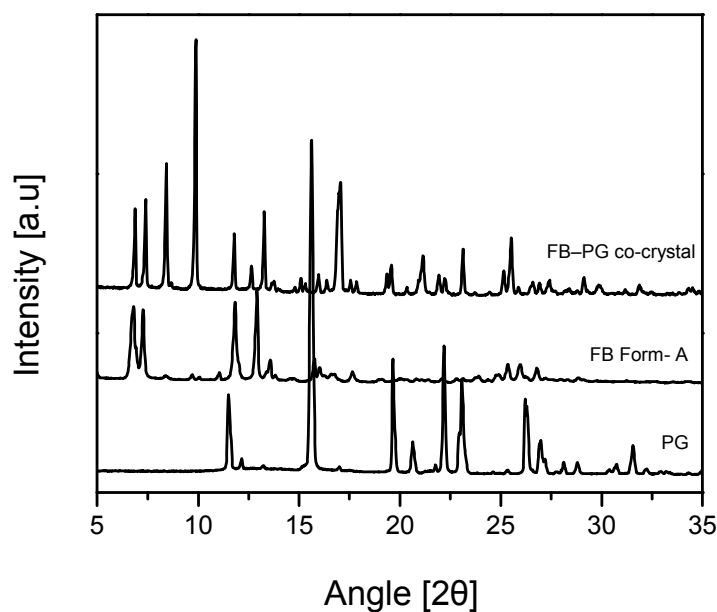


Figure 4. 2θ powder X-ray diffraction (PXRD) patterns of FB-PG cocrystal, FB form-A, and PG.

2.3. Prediction of FB-PG Cocrystal's Intermolecular Interactions Using Solid-State CP/MAS ^{13}C -NMR

Figure 5 illustrates overlapped solid-state CP/MAS ^{13}C -NMR spectra of FB-PG (2:1) cocrystal, FB, PG, and FB-PG (2:1) mixture. According to the data, the solid-state CP/MAS ^{13}C -NMR spectrum of FB-PG cocrystal was confirmed to be different from that of FB/PG mixture. Moreover, it was assumed that the solid-state CP/MAS ^{13}C -NMR spectrum of FB/PG solid mixture represents the overlapped solid-state CP/MAS ^{13}C -NMR spectra of FB form-A and PG (Figure 5). Further, a great difference was noticed in terms of peak intensity and sharpness between the solid-state CP/MAS ^{13}C -NMR spectrum of FB-PG cocrystal and FB/PG solid mixture. Also, the peaks of relatively great intensity and sharpness were observed on FB-PG cocrystal's solid state CP/MAS ^{13}C -NMR spectrum than on FB/PG mixture's solid-state CP/MAS ^{13}C -NMR spectrum. The observed difference is attributed to the difference in degree of crystallinity between these products. Therefore, it was assessed that FB-PG cocrystal possesses relatively excellent crystallinity [10].

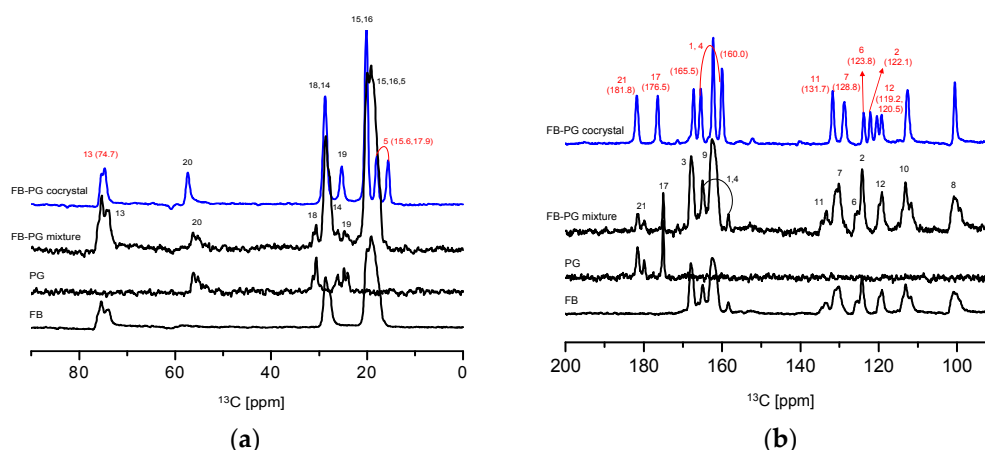


Figure 5. FB-PG (2:1) cocrystal, FB, PG, and FB/PG (2:1) mixture's solid-state CP/MAS ^{13}C -NMR spectra (a) 90 ppm–200 ppm; (b) 0 ppm–90 ppm (Numbers on the peaks are related to numbers in Figure 1 structure and peak location).

As can be seen in Figure 5 and Figure S3, both FB/PG mixture's solid-state CP/MAS ^{13}C -NMR spectrum and FB-PG cocrystal's solution-state ^{13}C NMR spectrum possess similar chemical shifts and identical patterns when their spectra are compared. Moreover, both solution-state ^{13}C -NMR spectra of FB-PG cocrystal and FB-PG mixture were found identical (Figure S3). Therefore, FB-PG cocrystal's solution-state NMR (^1H , ^{13}C) was used as a basis for the interpretation of the solid-state CP/MAS ^{13}C -NMR spectra (Figure 5). First, the solution-state 2D NMR spectra including ^1H - ^1H COSY, ^1H - ^{13}C HSQC, and ^1H - ^{13}C HMBC spectra were analyzed (Figures S3–S7). Through the ^1H - ^1H COSY analysis, the overall identification of every ^1H -NMR peaks observed on the spectrum was achieved. Afterwards, ^1H - ^{13}C HSQC analysis was performed for the identification of all peaks of carbon atoms covalently attached to protons. Finally, ^1H - ^{13}C HMBC analysis was conducted to identify the peaks of remaining carbon atoms. On the basis of the analyzed FB-PG cocrystal's solution-state ^{13}C NMR spectrum, the interpretation of both solid-state CP/MAS ^{13}C -NMR spectra of FB-PG cocrystal and FB/PG mixture was achieved. Afterward, the spectra were compared.

In Figure 5a it was observed that C2 located near the FB carboxylic acid (Figure 1a) undergoes an upfield in chemical shifts on the FB-PG cocrystal solid-state spectrum when compared with both FB-PG mixture's and FB-PG cocrystal's solution state spectra (Figure S3), which appears at 122.1 ppm. Moreover, C1 and C4 in FB undergo a downfield in chemical shifts on FB-PG cocrystal's solid-state spectrum compared to FB-PG mixture's and FB-PG cocrystal's solution-state spectra (Figure S3), and appear at 160.0 ppm and 165.5 ppm, respectively. This result coincided with the previously reported solid-state CP/MAS ^{13}C -NMR spectrum result of FB/*p*-aminobenzoic acid (PMBA) (1:1) cocrystal [17]. Similar to the above result, C2 located near FB carboxylic acid undergoes an upfield in chemical shifts while C1 and C4 undergo a downfield on FB/PMBA cocrystal's solid-state CP/MAS ^{13}C -NMR spectrum compared to FB form-A solid-state CP/MAS ^{13}C -NMR spectrum [17]. This result is attributed to the hydrogen bonding formed between the hydrogen bonding donor, FB carboxylic acid OH and the acceptor, C=O [17]. Accordingly, the action of OH and C=O functional groups of FB carboxylic acid as hydrogen bonding donor and acceptor is assumed to be responsible for the changes in chemical shifts of C1, C2, and C4 near the FB carboxylic acid in the Figure 5a. Moreover, as can be seen in Figure 5a, C6, C7, and C11 of FB aromatic ring (Ar) (Figure 1a) undergo an upfield in chemical shifts on FB-PG cocrystal solid state spectrum compared with the FB/PG mixture's and FB-PG cocrystal's solution state spectra (Figure S3), which appear in the interval between 123.8 ppm, 128.8 ppm, and 131.7 ppm.

Considering the above changes, it was possible to predict the intermolecular interactions between FB and PG. By considering the chemical shifts of the carbon atoms situated in FB carboxylic acid region,

it was presumed that carboxylic acid acts as hydrogen bonding donor and acceptor. Consistently, it was presumed that nitrogen acts as the hydrogen bonding acceptor due to the upfield of the chemical shift of the carbon atom located near by the nitrogen of FB thiazole ring. Furthermore, the overall changes in chemical shifts of PG's carbon atoms are attributed to the simultaneous actions of amide and carboxylic acid as hydrogen bonding donor and acceptor. Based on the above result, it was suggested that the hydrogen bonding including O–H···O and N···O–H that occur between FB and PG were responsible for the formation of FB-PG cocrystal. Besides, FT-IR analysis was performed to provide supporting evidence. The FT-IR analysis data shown in Figure 6 revealed that FB-PG cocrystal possesses a distinct FT-IR spectrum compared to FB form-A and PG. Great dissimilarities in wavenumber were observed in the region of NH-CO and COOH's carbonyl group from 1750 to 1610 cm^{-1} .

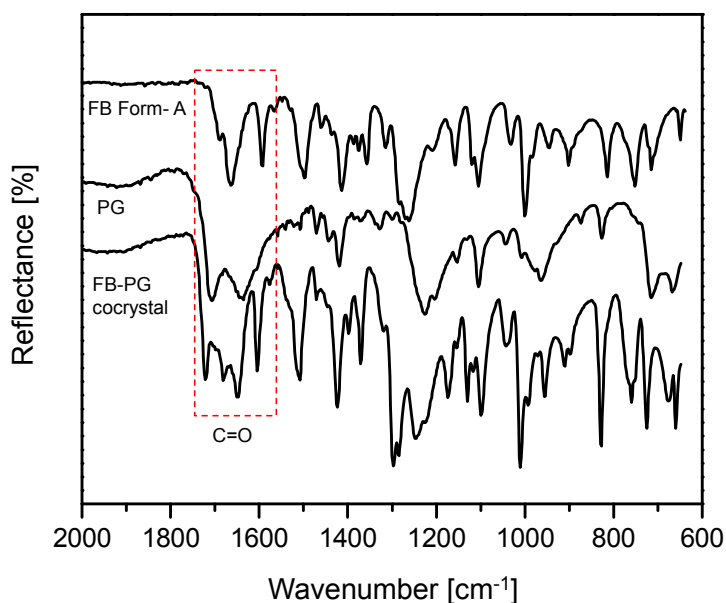


Figure 6. FT-IR spectra of FB-PG cocrystal, FB form-A, and PG.

According to the analysis, it was assessed that the hydrogen bonding occurring within FB-PG cocrystal in the region of carbonyl group was entirely different from the carbonyl group region in FB and PG (Figure 6).

Hence, it was assumed that the changes observed in carbonyl group region on the FT-IR spectrum (Figure 6) may serve as essential proof which can support the result regarding the prediction of FB-PG cocrystal's intermolecular interactions obtained using the solid-state CP/MAS ^{13}C -NMR spectrum illustrated in Figure 5a. It was also found out that functional groups forming hydrogen bonds in FB-PG cocrystal were identical with those forming hydrogen bonds in the five previously reported FB cocrystals [17,18]. This result confirms the predicted hydrogen bonding in FB-PG cocrystal through the results illustrated in Figure 5a. In Figure 5b, C5 represents the CH_3 of FB thiazole ring. The peak signal of C5 splits into two sub-peaks which appear at 15.6 ppm and 17.9 ppm. Besides, as can be seen, the peak of C13 corresponding to FB CH_2 splits into two sub-peaks observed at 74.7 ppm. Lastly, C12 peak signal, referring to $\text{C}\equiv\text{N}$, splitting in two sub-peaks at 120 ppm could be noticed in Figure 5a. Consequently, previously reported solid-state CP/MAS ^{13}C -NMR spectrum results of FB/saccharine (1:1) cocrystal and FB/acetamide (1:1) cocrystal are suggested as evidence to support the obtained result. Likewise, on these spectra, the peaks related to C5, C12, and C13 were splitted into two sub-peaks [17]. This is attributed to the possible existence of conformational isomers. Besides, further similarity in term of change in chemical shifts could be observed between the solid-state CP/MAS ^{13}C -NMR spectra of FB-PG cocrystal and the previously reported FB/saccharin (1:1) cocrystal [17]. Therefore, the formation of FB-PG cocrystal was suggested to be properly achieved. Moreover,

through FB-PG cocrystal solution-state $^1\text{H-NMR}$ spectrum analysis it was confirmed that FB-PG cocrystal is formed in FB and PG in 2:1 ratio (Figure 7). This result was also confirmed through FB-PG cocrystal's solution-state $^1\text{H-}^1\text{H}$ COSY analysis (Figure S6), FB, and PG's solution-state $^1\text{H-NMR}$ analysis (Figure S7), and analytical results of previously reported study [20–22].

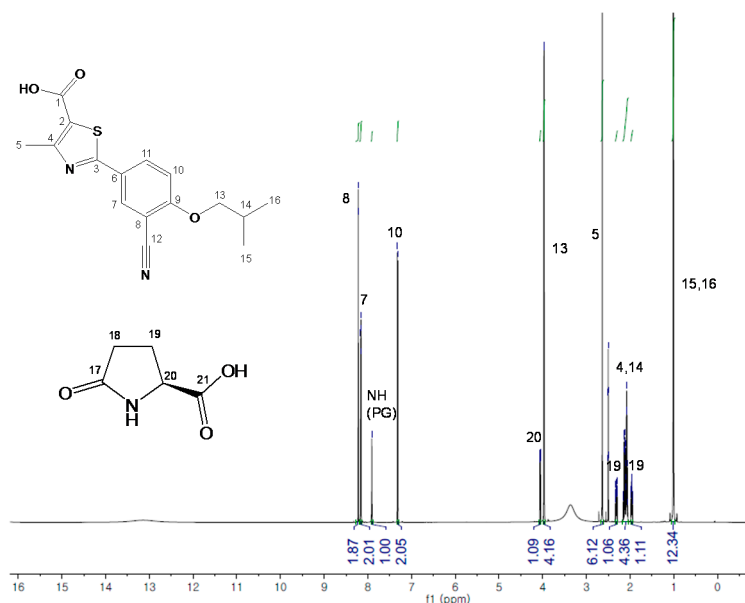


Figure 7. Integration of solution-state $^1\text{H-NMR}$ spectrum of FB-PG cocrystal (DMSO- d_6).

Through the results illustrated in Figures 3–7, it was assessed that the FB-PG cocrystal possesses a completely different crystal structure compared with FB form-A. Furthermore, the characterization of FB-PG cocrystals was confirmed.

2.4. Solubility of FB-PG Cocrystal

Table 2 represents the comparative solubility values of FB-PG cocrystal and FB form-A measured in deionized water and at gastrointestinal track pH (1.2, 4, and 6.8). According to the data, the solubility of FB-PG cocrystal in deionized water increased four-fold compared to FB form-A. Moreover, the solubility of FB-PG cocrystal was respectively two-fold and five-fold greater than FB form-A at pH 1.2 and pH 4.0, respectively. Alike its solubility in deionized water, the solubility of FB-PG cocrystal increased four times than FB form-A at pH 6.8.

As can be seen in Table 2, the drawback regarding the low water-solubility of FB form-A was greatly enhanced with FB-PG cocrystal. Consequently, FB-PG cocrystal is assumed as potential API possessing the ability to improve the solubility and absorption rate and bioavailability of FB form-A.

Table 2. Solubility comparison of FB-PG cocrystal and FB form-A in water and at pH 1.2, 4, and 6.8.

	FB form-A [$\mu\text{mol/mL}$]	FB-PG Cocrystal [$\mu\text{mol/mL}$]
water	0.041	0.161
pH 1.2	1.337	2.605
pH 4.0	0.129	0.670
pH 6.8	0.041	0.170

3. Materials and Methods

3.1. Materials

Febuxostat form-A (purity 99.56%) and amino acids (Table 1) were provided by the pharmaceutical raw material company, J2H biotech. Co., Ltd., (Ansan, Korea). In addition, methanol, ethanol, isopropyl alcohol, n-hexane, dichloromethane, and acetone applied in this experiment were purchased from DaeJung Chem. Co., Ltd. (purity > 99%) (Siheung, Korea).

3.2. Production of FB-PG Cocrystal by Using Liquid-Assisted Grinding Technique

For the screening experiment, FB 1 g and amino acid (Table 1) 1 eq. were combined in a mortar and then the materials were ground using a pestle throughout 50 min with the addition of 1 drop of solvent (MeOH, EtOH, IPA, Hex, DCM, and ACT) every 10 min. As a result, cocrystal was obtained when FB and PG were combined and ground with the addition of two drops of ACT every 10 min. Accordingly, FB 10 g and PG 2.1 g (0.55 equivalent) were placed together in a mortar and then ground with pestle for 50 min with the addition of three drops of ACT every 10 min to produce FB-PG (2:1) cocrystal.

3.3. Solid-State Nuclear Magnetic Resonance Spectroscopy (Solid-State CP/MAS ^{13}C -NMR)

The solid-state CP/MAS ^{13}C -NMR spectra of FB-PG cocrystal powder and FB-PG mixture (2:1) were recorded on a 500 MHz solid-state NMR (Avance II, Bruker, Billerica, MA, USA). The spectral acquisition was achieved using the cross polarization (CP)/magic angle spinning (MAS) pulse sequence. The measurement conditions were; spinning 5 KHz, pulse delay 5 s, contact time 2 ms, and 24 hs analysis time per sample.

3.4. Solution-State Nuclear Magnetic Resonance Spectroscopy (Solution-State NMR)

1D (^1H and ^{13}C) and 2D (COSY, HMQC, and HMBC) analyses of FB-PG cocrystal, FB form-A and PG were performed on 800 MHz High Resolution NMR Spectrometer (Avance, Bruker, Billerica, MA, USA). FB-PG cocrystal, FB form-A, and PG were dissolved in DMSO- d_6 prior to analysis.

3.5. Attenuated Total Reflectance Fourier Transform Infrared Spectroscopy (ATR-FTIR)

ATR-FTIR (PerkinElmer Spectrum 100 FT-IR spectrometer with a PerkinElmer Universal ATR Sampling Accessory (Boston, MA, USA)) was employed for the assessment of hydrogen-bonding within FB-PG cocrystal. The spectral range was set from 4000 to 650 cm^{-1} , the resolution was set to 4, while the number of scans was 150.

3.6. Powder X-ray Diffraction (PXRD)

Powder X-ray diffractometer (Bruker, D8 Advance, Billerica, MA, USA) was employed to investigate the crystallographic characteristics of FB-PG cocrystal. Here, the diffraction patterns were measured in 2θ , the scan rate was $5^\circ/\text{min}$, and the scan range was set from 5° to 35° .

3.7. Differential Scanning Calorimetry (DSC)

DSC (Q20, TA Instruments, Philadelphia, PA, USA) was used for the thermal analysis of FB-PG cocrystal. The scan rate was $10^\circ\text{C}/\text{min}$ and the heat range was set from 20 to 250°C .

3.8. Solubility Test

The water solubility and the effect of pH on the solubility of FB-PG cocrystal and FB form-A were measured using a HPLC (Agilent 1100, Santa Clara, CA, USA). A C_{18} column (4.6×150 mm, $5 \mu\text{m}$, Kromasil[®], Bohus, Sweden) was used, and the mobile phase composition was 10 mM ammonium acetate (pH 4.0): acetonitrile = 15:85 (v/v). The sample running time was 15 min with a flow rate of 1 mL/min. Samples were monitored using UV absorbance at 275 nm. Samples were diluted 100-fold

into acetonitrile prior to HPLC analysis. To determine the effect of pH on the solubility of samples, the FB-PG cocrystal and FB form-A were dissolved in buffer solutions of pH 1.2, pH 4, and pH 6.8.

4. Conclusions

The present study was carried out in the aim of producing new FB cocrystal to enhance the water solubility of the poorly water-soluble drug FB form-A. Five amino acids were used for screening experiments to produce cocrystals of FB. As the result, an FB-PG (2:1) cocrystal was obtained, and by means of solid-state CP/MAS ^{13}C -NMR analysis, the intermolecular interactions present in FB-PG cocrystals were predicted. According to the data analysis, it is assumed that the OH group of carboxylic acid in FB acts as a donor, whereas the nitrogen of thiazole group in FB acts as an acceptor to achieve hydrogen bond between FB and PG. Thus, it could be presumed that $\text{O}-\text{H}\cdots\text{O}$ and $\text{N}\cdots\text{O}-\text{H}$ hydrogen bonds are the intermolecular interactions responsible for the formation of cocrystal. Additionally, a comparative solubility test between FB-PG cocrystal and FB form-A conducted in deionized water and simulated gastrointestinal pH (1.2, 4, and 6.8) revealed that the solubility of FB-PG cocrystal increased up to four times compared to FB form-A in deionized water and up to two and five times than FB form-A at simulated gastrointestinal pH 1.2 and pH 4, respectively. Solubilities of FB-PG cocrystal and FB form-A at pH 6.8 were similar to those measured in deionized water.

As regards the results, it can be confirmed that FB-PG cocrystal was able to overcome the water-solubility drawback of FB form-A. Consequently, FB-PG cocrystal was presumed as potential API possessing the enhanced absorption property compared to FB form-A.

Supplementary Materials: The following are available online at www.mdpi.com/2073-4352/7/12/365/s1, Table S1. Comparison of the 2θ angle data of the FB-PG cocrystal and FB polymorphs; Table S2. Comparison of the 2θ angle data of the FB-PG cocrystal, FB and PG; Figure S1. DSC curve of FB form-A (heating rate $10\text{ }^\circ\text{C}/\text{min}$); Figure S2. DSC curve of PG (heating rate $10\text{ }^\circ\text{C}/\text{min}$); Figure S3. Solution-state ^{13}C -NMR data of FB/PG (2:1) mixture and FB-PG cocrystal ($\text{DMSO}-d_6$); Figure S4. Solution-state 2D (^1H - ^{13}C HSQC) NMR data of FB-PG cocrystal ($\text{DMSO}-d_6$); Figure S5. Solution-state 2D (^1H - ^{13}C HMBC) NMR data of FB-PG cocrystal ($\text{DMSO}-d_6$); Figure S6. solution-state 2D (^1H - ^1H COSY) NMR data of FB-PG cocrystal ($\text{DMSO}-d_6$); Figure S7. FB and PG's solution-state ^1H -NMR data ($\text{DMSO}-d_6$) (a) FB, (b) PG.

Acknowledgments: This research was supported by the Basic Science Research Program through the National Research Foundation of Korea (NRF) funded by the Ministry of Education (NRF-2016016008). The Gyeonggi GRRRC program (GRRRC-CHA2017-A01) is acknowledged for supporting the NMR analysis.

Author Contributions: Ji-Hun An and Changjin Lim performed the bulk of the experimental work. Alice Nguvoko Kiyonga, Minho Park and Hyuk Min Kim performed some experiments. Hyung Chul Ryu and Jae Sun Kim contributed materials. Kiwon Jung and Gyu Hwan Park designed and supervised the work. Ji-Hun An, Alice Nguvoko Kiyonga, Minho Park, Changjin Lim, Young-Ger Suh, and Kiwon Jung analyzed the data and wrote the manuscript.

Conflicts of Interest: The authors declare no conflict of interest.

References

1. Hilfiker, R. *Polymorphism in the Pharmaceutical Industry*; Wiley-Vch: Weinheim, Germany, 2006; pp. 1–15.
2. Chen, J.; Sarma, B.; Myerson, A.S. Pharmaceutical crystallization. *Cryst. Growth Des.* **2011**, *11*, 887–895. [[CrossRef](#)]
3. Sparma, B.; Chen, J.; His, H.Y.; Myerson, A.S. Solid form of pharmaceuticals: Polymorphs, salt and cocrystals. *Korean J. Chem. Eng.* **2011**, *28*, 315–322. [[CrossRef](#)]
4. Babu, N.J.; Nangia, A. Solubility advantage of amorphous drugs and pharmaceutical cocrystals. *Cryst. Growth Des.* **2011**, *11*, 2662–2679. [[CrossRef](#)]
5. Reddy, L.S.; Babu, N.J.; Nangia, A. Carboxamide-pyridine N-oxide heterosynthon for crystal engineering and pharmaceutical cocrystals. *Chem. Commun.* **2006**, *13*, 1369–1371. [[CrossRef](#)] [[PubMed](#)]
6. Bhogala, B.R.; Basavoju, S.; Nangia, A. Three-component carboxylic acid-bipyridine lattice inclusion host. Supramolecular synthesis of ternary cocrystals. *Cryst. Growth Des.* **2005**, *5*, 1683–1686. [[CrossRef](#)]

7. Reddy, L.S.; Basavoju, S.; Vangala, V.R.; Nangia, A. Hydrogen bonding in crystal structures of *N,N'*-Bis(3-pyridyl) urea. Why is the NH tape synthon absent in diaryl ureas with electron-withdrawing groups? *Cryst. Growth Des.* **2006**, *6*, 161–173. [[CrossRef](#)]
8. Aakeröy, C.B.; Hussain, I.; Desper, J. 2-Acetaminopyridine: A highly effective cocrystallizing agent. *Cryst. Growth Des.* **2006**, *6*, 474–480. [[CrossRef](#)]
9. Chadha, R.; Bhalla, Y.; Vashisht, M.K.; Chadha, K. *Recrystallization in Materials Processing*; Intech: Vienna, Austria, 2015; pp. 173–174.
10. Harris, R.K. Application of solid-state NMR to pharmaceutical polymorphism and related matters. *J. Pharm. Pharmacol.* **2007**, *59*, 225–239. [[CrossRef](#)] [[PubMed](#)]
11. Vogt, F.G.; Clawson, J.S.; Strohmeier, M.; Edwards, A.J.; Pham, T.N.; Watsom, S.A. Solid-State NMR analysis of organic cocrystals and complexes. *Cryst. Growth Des.* **2009**, *9*, 921–937. [[CrossRef](#)]
12. Mandala, V.S.; Loewus, S.J.; Mehta, M.A. Monitoring cocrystal formation via in situ solid-state NMR. *J. Phys. Chem. Lett.* **2014**, *5*, 3340–3344. [[CrossRef](#)] [[PubMed](#)]
13. Sokal, A.; Pindelska, E.; Szeleszczuk, L.; Kolodziejski, W. Pharmaceutical properties of two ethenzamide-gentic acid cocrystal polymorphs: Drug release profiles, spectroscopic studies and theoretical calculations. *Int. J. Pharm.* **2017**, *522*, 80–89. [[CrossRef](#)] [[PubMed](#)]
14. Matsumoto, K.; Watanabe, K.; Hiramatsu, T.; Kitamura, M. Polymorphs of 2-(3-cyano-4-isovutyloxyphenyl)-4-methyl-5-thiazolecarboxylic Acid and Method of Producing the Same. U.S. Patent 6225474 B1, 1 May 2001.
15. Iwai, M.; Nakamura, K.; Dohi, M.; Mochizuki, H.; Mochizuki, S. Solid Preparation Containing Single Crystal Form. U.S. Patent 7361676 B2, 22 April 2008.
16. Jiang, Q.Y.; Qian, J.J.; Gu, J.M.; Tang, G.P.; Hu, X.R. Febuxostat methanol solvate. *Acta Cryst.* **2011**, *E67*, 1232. [[CrossRef](#)] [[PubMed](#)]
17. Maddileti, D.; Jayabun, S.K.; Nangia, A. soluble cocrystals of the xanthine oxidase inhibitor febuxostat. *Cryst. Growth Des.* **2013**, *13*, 3188–3196. [[CrossRef](#)]
18. Wu, M.; Hu, X.R.; Gu, J.M.; Tang, G.P. Crystal structure of febuxostat-acetic acid (1/1). *Acta Cryst.* **2015**, *E71*, 295–296. [[CrossRef](#)] [[PubMed](#)]
19. Stahl, P.H.; Wermuth, C.G. *Handbook of Pharmaceutical Salt Properties, Selection, and Use*; Wiley-Vch: Weinheim, Germany, 2002; pp. 272–320.
20. Vallu, V.R.; Desai, K.G.; Patil, S.D.; Agarwal, R.; Padi, P.R.; Ghanta, M.R. Synthesis and characterization of some analogues of Febuxostat—An anti-hyperuricemia drug. *ACAIJ* **2014**, *14*, 339–350.
21. Vallu, V.R.; Desai, K.G.; Patil, S.D.; Agarwal, R.; Padi, P.R.; Ghanta, M.R. Synthesis and characterization of process-related impurities of an anti-hyperuricemia drug-Febuxostat. *Der Pharma Chem.* **2014**, *6*, 300–311.
22. Yoshifuji, S.; Tanaka, K.I.; Kawal, T.; Nitta, Y. A novel of L-pyroglutamic acid derivatives from L-proline: utility of *N*-protecting groups for ruthenium tetroxide oxidation of cyclic α -amino acids. *Chem. Pharm. Bull.* **1986**, *34*, 3873–3878. [[CrossRef](#)]

